Hindawi
The Scientific World Journal
Volume 2021, Article ID 6685045, 18 pages
https://doi.org/10.1155/2021/6685045

Research Article

Analysis of the Current and Future Prediction of Land Use/Land Cover Change Using Remote Sensing and the CA-Markov Model in Majang Forest Biosphere Reserves of Gambella, Southwestern Ethiopia

Semegnew Tadese,[1] **Teshome Soromessa**,[1] **and Tesefaye Bekele**[2]

[1]*Addis Ababa University, Center of Environmental Sciences, Addis Ababa, Ethiopia*
[2]*Ethiopian Environments and Forestry Research Institute, Addis Ababa, Ethiopia*

Correspondence should be addressed to Semegnew Tadese; semetade@gmail.com

Received 23 November 2020; Revised 16 January 2021; Accepted 6 February 2021; Published 23 February 2021

Academic Editor: Syed Abbas

This study aimed to evaluate land use/land cover changes (1987–2017), prediction (2032–2047), and identify the drivers of Majang Forest Biosphere Reserves. Landsat image (TM, ETM+, and OLI-TIRS) and socioeconomy data were used for the LU/LC analysis and its drivers of change. The supervised classification was also employed to classify LU/LC. The CA-Markov model was used to predict future LU/LC change using IDRISI software. Data were collected from 240 households from eight kebeles in two districts to identify LU/LC change drivers. Five LU/LC classes were identified: forestland, farmland, grassland, settlement, and waterbody. Farmland and settlement increased by 17.4% and 3.4%, respectively; while, forestland and grassland were reduced by 77.8% and 1.4%, respectively, from 1987 to 2017. The predicted results indicated that farmland and settlement increased by 26.3% and 6.4%, respectively, while forestland and grassland decreased by 66.5% and 0.8%, respectively, from 2032 to 2047. Eventually, agricultural expansion, population growth, shifting cultivation, fuel wood extraction, and fire risk were identified as the main drivers of LU/LC change. Generally, substantial LU/LC changes were observed and will continue in the future. Hence, land use plan should be proposed to sustain resource of Majang Forest Biosphere Reserves, and local communities' livelihood improvement strategies are required to halt land conversion.

1. Introduction

Land cover and land use represent the assimilating elements of the resource base. Land use describes activities, arrangements, and inputs often associated with people that take place on the land and represent the current use of property such as residential homes, shopping centres, row crops, tree nurseries, state parks, and reservoirs. Land cover describes the natural and anthropogenic features that can be observed on the Earth's surface, i.e., forests, tidal wetlands, developed/built areas, grasslands, and water [1–3]. Land use/land cover (LULC) change is perhaps the most important concern in many regions of the world [4–7]. It is recognized that dramatic LULC change can significantly impact regional climate, ecosystem stability, water balance, stream silt up, socioeconomic practices, and biodiversity [8–14]. As the pressure of the LULC change is increasing in many places, understandings of current and future LULC changes and patterns are a critical issue and seek timely analysis [8, 9, 15]. LU/LC change is significantly increasing and primarily activated by natural phenomena and anthropogenic activities [10, 11]. To collect information and time serious LU/LU change, ground surveys and satellite sensors can be utilized [12].

Prediction of LU/LC using time serious data is important for the future management plan of LULC [13], and it is regularly employed for a diverse suitability measure as a proxy of human influence on land change processes. A

Markov model is one in which the future state of a system can be predicted purely based on the proximately preceding state. Predicting future change is achieved by creating a transition probability matrix of LULC change from period one to period two [14]. Multispectral satellite images and the CA-Markov chain model were used by the researcher to predict the LULC change in different regions [16–18]. It also computed states between different land uses and quantified the transition rate between different land uses [19]. The factors in which driving forces of LULC change were combined to provide the estimation of future scenarios [20].

In Ethiopia, LULC changes are a persistent event where agricultural activities and settlements are dominated in the rural landscapes. Recent studies indicated that land use/land cover change is increasing; predominantly, expansion of agricultural land at the expense of natural forest was observed in different parts of Ethiopia [8, 13, 15, 21–31]. For instance, Kindu et al. [8] reported that about 66.2% of woodland converted to farmland in Munessa-Shashemene of Oromia, Ethiopia. However, nearly 27% increase of forest cover was gained as results of community afforestation and rehabilitation activities on degraded hilly lands in Chemoga watershed within the Blue Nile, Ethiopia [32, 33].

Moreover, LULC changes analysis has been conducted to identify driving forces of the changes in different parts of Ethiopia [13, 27, 34–37]. For example, a study from Afar region identified more than fifteen LULC changes driving factors such as migration triggered by drought, land tenure, and government policy changes [34]. The study from the central rift valley revealed that population growth, a decline in agricultural productivity, land tenure change, and erratic rainfall are the major drivers of LULC changes in the study area [37]. Likewise, driving factors of LULC changes are diverse in different places or regions. Hence, driving factors of LULC changes of certain ecosystems or places should be addressed and investigated locally based on the agroecology and socioeconomic condition of the area.

Analysis and prediction of LULC changes have significant roles in the understanding of earth-atmosphere interaction, forest fragmentation, biodiversity loss, and future management plans [9, 38–41]. Also, inspection and analysis of LULC have greatly increased in providing the most accurate evaluation of the world's forest, grassland, and agricultural resources regarding their spread status and health [42]. However, studies concerning LULC changes, drivers, and prediction have not been performed in Majang Zone, a place where the UNSECO registered forest biosphere reserve was established recently. The objectives of this study are to analyse LU/LC changes over the last three decades 1987–2017, predict future LU/LC change from 2017 to 2047, and identify LU/LC changes drivers of the Majang Forest Biosphere Reserve (MFBR).

2. Materials and Methods

2.1. Description of the Study Area. This study was conducted in Majang Forest Biosphere Reserve (MFBR) which is found in the Majang Zone, Gambella National Regional State of Ethiopia. It is unique biogeography and shares a border with Illubabor Zone of Oromia Regional State and Sheka and Bench-Maji zones of the Southern Nations, Nationalities, and People (SNNP). It covers a total area of 233,254 ha of forest, woodland, agricultural land, rural settlement, and towns (Figure 1). MFBR is located between 07°08′-07°23′ latitude and 035°04′-035°19′ longitude, and the area has an altitude range of 562–2444 m [1].

The climate of the zone is generally characterized by a hot and humid type, which is marked on most rainfall maps of Ethiopia as being the wettest part of the country (Figure 2). The annual average rainfall is 1774, and means annual minimum and maximum monthly temperature ranges between 13.9°C and 31.8°C in Tinishu Meti Metrological Station (Figure 2(a)). The annual average rainfall is 2053, and mean annual minimum and maximum monthly temperature ranges between 11.8°C and 29.7°C in Ermichi Metrological Station (Figure 2(b)). The maximum average monthly temperature is in February (29.8°C and 31.8°C) while the minimum is in January (11.9°C and 13.9°C), in Ermichi and Tinishu Meti, respectively. The maximum rainfall is between April and October and low rainfall from November to March (NMSA, 2019) (Figure 2).

The major vegetation types of the forest biosphere reserves are Montana evergreen forest, lowland semievergreen forest, and riparian vegetation (WBISPP, 2000). Besides, the vegetation of this area has different categories in terms of life forms such as a high natural forest, woodlands, bushlands, and grasslands which are the major vegetation types in the forest biosphere reserves, and it is categorized under moist Afromontane forest among four Ethiopian biome categories (MEFCC, 2017).

2.2. Data Acquisition and Processing. Freely available satellite imagery (Landsat-5 TM (1987), Landsat-7 ETM+ (2002), and Landsat-8 OLI-TIRS (2017)) was downloaded from the USGS website https://earthexplorer.usgs.gov/ of Earth explorer. These data were projected to Universal Transverse Mercator (UTM) with a datum of the World Geodetic System 84 (WGS84), projection system zone 36 N (Table 1). Dataset selection was fixed in the dry season when a clear sky period occurs in which the lowest or zero monthly cloud cover is achieved.

Atmospheric correction (FLAASH module), geometric correction, mosaicking, and masking were performed during preprocessing using ENVI version 5.3 before classifying the images [35, 36]. Atmospheric correction and geometric correction were used to avoid sensor noise, haze, adjustment of data loss, and missing line because of solar position and satellite calibration [43].

Prior to image classifications, ground reference points (GRP) were collected through direct field observation to verify classified images with land use/cover type. The total numbers of GRP collected in the study area were 250, with 50 GRP for each LU/LC type using a global positioning system (GPS). Pixel-based supervised image classification with the maximum likelihood classification (MLC) algorithm [19, 20, 37] was carried out for image classification of the study periods. In supervised classification, region of

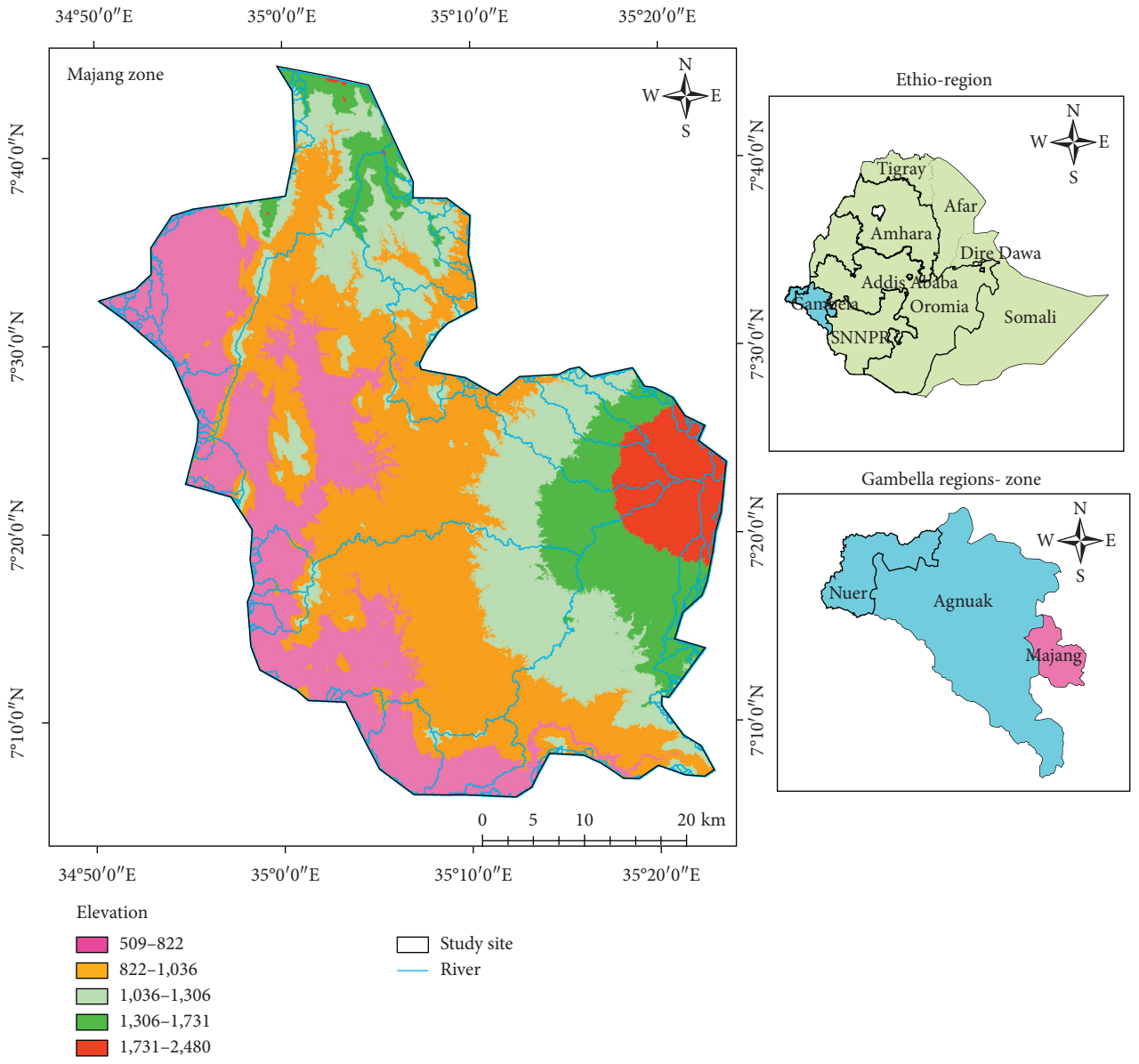

Figure 1: Location of the study area.

interest (ROI) was applied as a signature for each land use class. A total of 300 ROI signatory was made with the maximum number of ROI in forestland (90) and the minimum number in waterbody (30).

Based on the existing feature of LULC in the study area landscape, the Coordination of Information on the Environment (CORINE) LULC classification system was used to classify the LULC classes [44]. Therefore, we classified LULC into five classes: forestland, farmland, grassland, settlement, and waterbody. The LULC classes together with their description are presented in Table 2. ENVI 5.3 and Arc GIS 10.4.1 softwares were used to image classification.

The accuracy assessments were accomplished for classified images of 1987, 2002, and 2017 by applying a minimum of 40 random points created as per class with stratified random sampling, for which the corresponding reference classes of each LULC class were collected by field visit [46, 47]. Then, the accuracy assessments were computed using a confusion matrix (ground truth ROI). Therefore, the results of the accuracy assessment of the classified image showed an accuracy of 85.5%, 86%, and 87.3%, and Kappa statistics were in the range of 0.81–0.83% for the years 1987, 2002, and 2017, respectively (Table 3).

2.3. Suitability LU/LC and Input Data Preparation. The classified maps were reclassified considering the priority of suitability for each LULC class, and each reclassifies map was weighted and overlayed by including factors such as distance to road, slope, and altitude in Arc GIS. The constraints are a condition that limits the expansion of LULC classes. The factors give a degree of suitability for an area to be changed. The constraints and factors considered were distance to road, elevation, and slope suitable areas for conversion to

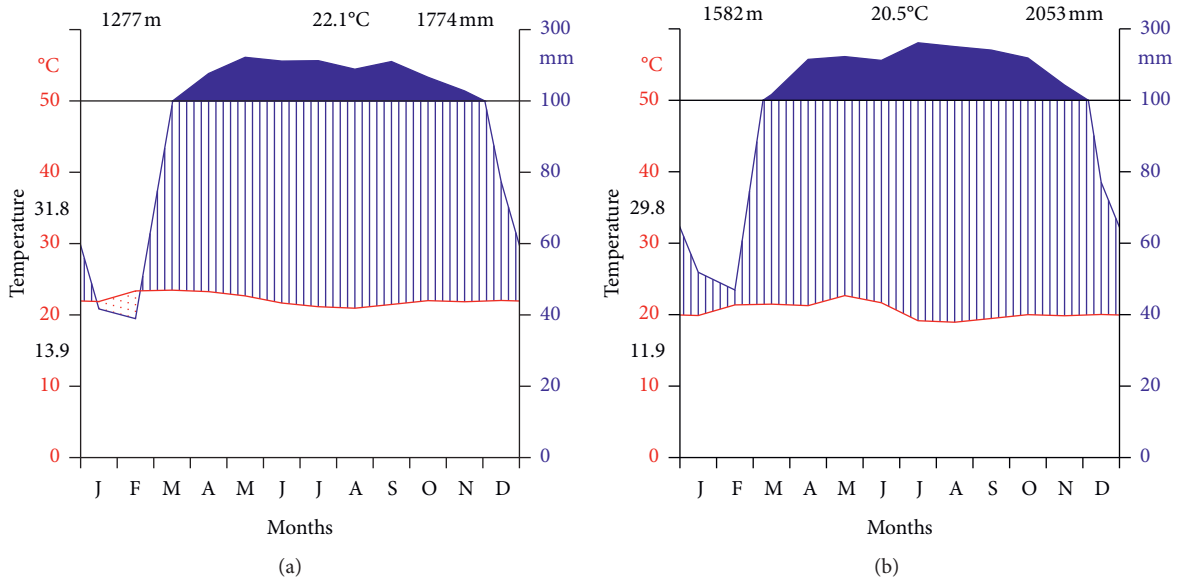

Figure 2: Mean annual temperature and rainfall recorded in (a) Tinishu Meti (1987–2017) and (b) Ermichi (1987–2017) Metrological stations.

Table 1: Satellite images used for LULC change analysis and their characteristics.

Satellite image	Path/Row	Sensor	Resolution (m)	No. of bands	Date of acquisition	Cloud cover
Landsat-5	170/55	TM	30	7	01/22/1987	0
	171/55	TM	30	7	01/31/1987	0
Landsat-7	170/55	ETM+	30	8	12/28/2002	0
	171/55	ETM+	30	8	12/19/2002	0
Landsat-8	170/55	OLI-TIRS	30	11	01/08/2017	0
	171/55	OLI-TIRS	30	11	01/15/2017	0

Table 2: Description of the LULC classification system.

LULC	Description
Forestland	Land covered with trees reaching 5 m in height, 0.5 ha in area, and a canopy cover of >10%.
Farmland	Areas covered with annual and perennial crops
Settlement	These areas both in urban and small rural residential places including trees in individual garden and big and small size roads
Grassland	Areas dominantly covered with grasses and shrubs
Waterbody	Waterbody: area which holds water (lakes), rivers, and marshy land

Source: [45].

Table 3: Accuracy assessment of 1987, 2002, and 2017 classified images.

Land use/land cover	1987		2002		2017	
	Producer accuracy	User accuracy	Producer accuracy	User accuracy	Producer accuracy	User accuracy
Forestland	86.3	92	87.8	90.2	89	91.9
Farmland	86.7	85.68	89.33	82.2	90	85.78
Grassland	71.6	84.5	75	80.9	80.5	79.9
Settlement	80.7	89	81.6	85.9	83.4	81.7
Waterbody	79.6	81	84.4	83.8	85.7	82
Overall accuracy (%)	85.4		86		87.3	
Kappa coefficient	0.81		0.82		0.83	

each class. The constraints are articulated in the Boolean maps where the suitable areas were set a value of 1, while the area not suitable was set a value of 0 [48]. The factors were changed to binary format from 0 to 255, in which 255 is highly suitable and 0 is not suitable using IDRISI version 17.0 for further processing.

The suitability maps (forestland, farmland, grassland, settlement, and waterbody) were derived using the Decision Wizard module in IDRISI (Figure 3). First, the constraints were standardized into Boolean maps, and then, the fuzzy function combined with the weighted linear combination (WLC) was used to process the standard factors. The factors were stretched from 0 to 255 with fuzzy function (sigmoidal), by monotonically increased control point. The weights of the factors resulted from the AHP function in the WLC module. Then, the transition suitability maps of all classes were made in the MCE module using the constraints, factors, and weights. Finally, the suitability and factors images were used as an input in the Markov change prediction model.

2.4. Simulation of LULC Change Using the CA-Markov Chain Model (CA-MCM). A CA-Markov model is applied to use both special and temporal LULC changes modelling [49, 50]. The CA-Markov model combines cellular automata and Markov chain to predict the characteristics and trends of LULC change over time, provide a better understanding of the factors that drive forest changes, and generate future land use/land cover scenarios to support the design of policy responses [22, 51, 52]. Moreover, this model is commonly used to illustrate the dynamics of LULC, forest cover, settlement expansion, plant growth, and modelling of watershed management. It is also significant to land use policy design and planning for sustainable land use development [53]. Therefore, it is essential to study the chronological LULCC to understand the relations between humans and the environment from a long-term view [51].

To predict future LULC changes for the study site, IDRISI software version 17 (CA-Markov model) was used. While doing so, the following specific processes were followed: (a) LU/LC maps for the years 1987 and 2017 were used to obtain the transition probabilities image [52, 54]. (b) Considering the CA-Markov model approach, the LULC for the year 2017 was simulated using the transition probabilities of the year 1987–2002. (c) The transition suitability image was computed using constraints and factors in the multicriteria evaluation (MCE) module [55–57]. (d) Finally, the LULC for the year 2032 and 2047 were projected using the transition probabilities images, base map, and transition suitability image (Figure 4).

2.4.1. CA-Markov Chain Model (CA-MCM) Approach. The CA-Markov model is the integration of cellular automata and transition probability matrix created by the cross-tabulation of two dissimilar images [58]. This integration of the CA-Markov model offers a strong method in spatial and temporal dynamic modelling [58, 59]. In other words, the CA-Markov chain can simulate and predict any transitions among any number of categories [60, 61]. CA is a dynamic procedure model that is frequently used in a spatial model for predicting future land use/land cover change [61–63]. The important properties of CA are that they show the spatial and dynamic process and that is why they have been broadly used in land use/land cover simulation [61]. The CA model is shown in the following equation (1) [53, 64, 65].

$$S\,(t,\, t+1) = f\,(S(t),\, N), \tag{1}$$

where $S\,(t+1)$ is the system status at the time of $(t,\ t+1)$, functioned by the state probability of any time (N).

The Markov chain model is often used in LULC monitoring, ecological modelling, simulation changes, trends of the LULC, and to predict the extent of the land use change and the stability of future land development in the area of concern [50, 62, 65]. The Markov chain model pronounces the LULC change from one time to another to predict future change [66, 67]. Equation (1) explains the calculation of the prediction of LULC changes (Markov chain model):

$$S(t, t+1) = P\text{ij} \times S(t), \tag{2}$$

where $S\,(t)$ is the system status at the time of t, $S\,(t+1)$ is the system status at the time of $t+1$; Pij is the transition probability matrix in a state which is calculated as follows [19, 66]:

$$= \left\| P_{\text{ij}} \right\| = \begin{Vmatrix} P1,1 & P1,2 & P1,N \\ P1,1 & P2,2 & P2,N \\ \cdots & \cdots & \cdots \\ \text{PN},1 & \text{PN},2 & \text{PN},N \end{Vmatrix}, \tag{3}$$

$$\left(0 \le P_{\text{ij}} \le 1\right), \tag{4}$$

where P is the transition probability; P_{ij} stands for the probability of transforming from present state i to another state j in succeeding time; PN is the state probability of any time. The high transition has probabilities near (1) and the low transition will have a probability near (0) [66]. Markov Chain concludes precisely how much land would be estimated to change from the latest date to the predicted date. The transition probabilities file is the result of this process, which is a matrix that registers the probability that each land use/land cover class will change to every other class [68].

2.4.2. CA-Markov Model Validation Approach. The use of kappa indexes for the calculation determines the overall achievement rate, and it delivers an understanding of the real factors in the strength or weakness of the results. When 75% ≤Kappa <100, the result maps are in a high level of agreement; if 50% ≤Kappa ≤75%, the result maps are in a medium level of agreement; and if Kappa ≤50, the result maps are in a poor agreement [69, 70]. Therefore, to know the accuracy of the CA-Markov model in simulating future LULC conditions, the model was confirmed [55] after simulating the 2017 LULC situations using the 1987 and 2002 classified images. Kappa index of agreement (K_{IA}) [71] such as Kappa for no information (K_{no}), Kappa for location (K_{location}), and Kappa for standard (K_{standard}) [55, 71] evaluated the agreements of the two maps (actual and simulated 2017) using the CROSSTAB Module in IDRISI. Besides, comparisons of the simulated and the actual area of each LULC class were also performed using the validate

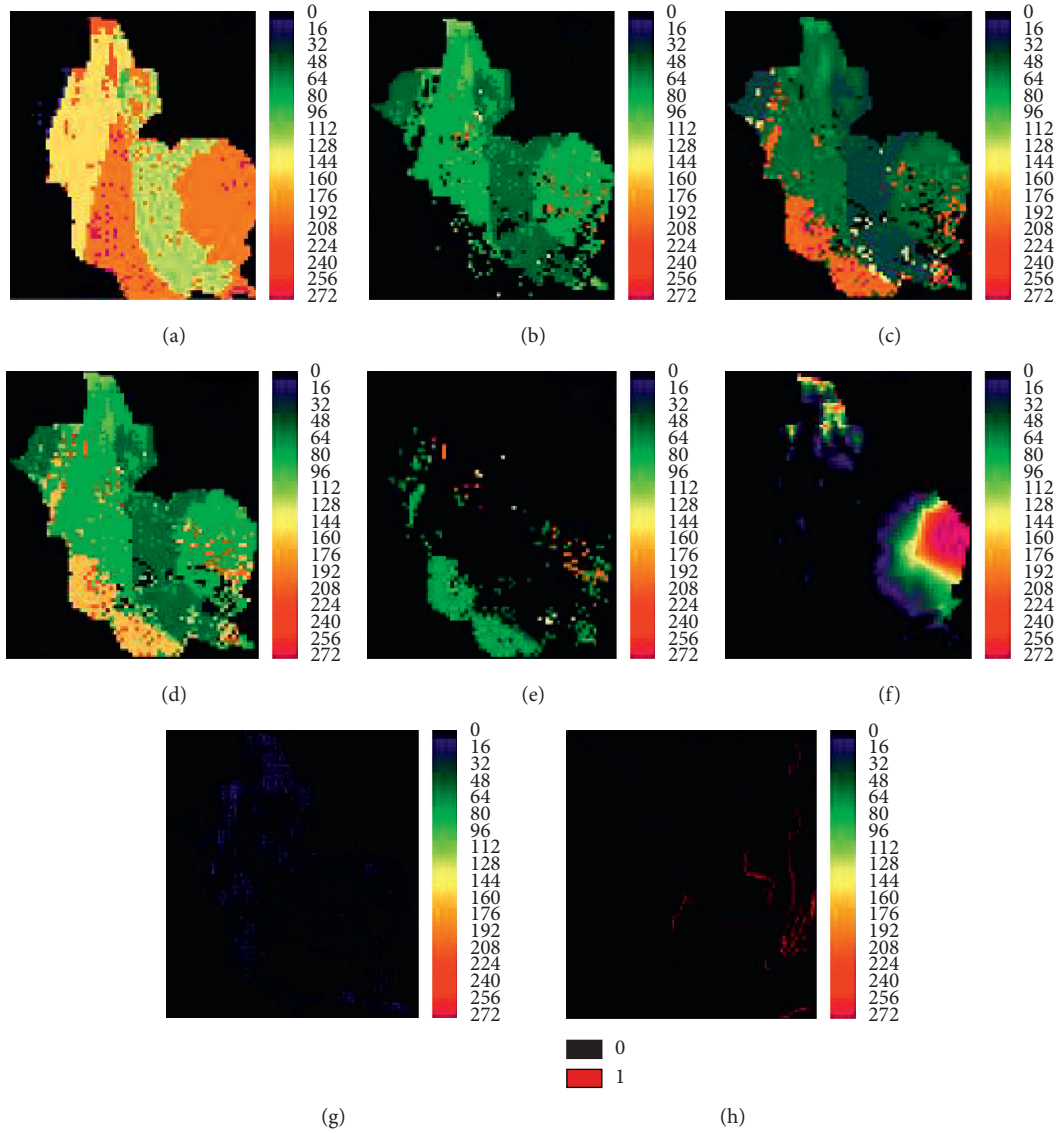

Figure 3: The suitability maps and input data: forestland (a), farmland (b), grassland (c), settlement (d), and waterbody (e) are suitability maps. Elevation (f), slope (g), and road (h) are the input data.

module. Hence, the kappa index is acceptable; the land use and land cover in 2032 and 2047 can be predicted. The following equations express the statistics for the kappa variations according to Omar et al. [55]:

$$K_{\text{no}} = \frac{(M(m)N(n))}{P(p) - N(n)},$$

$$K_{\text{location}} = \frac{(M(m)N(n))}{P(p) - N(n)}, \quad (5)$$

$$K_{\text{standard}} = \frac{(M(m)N(n))}{P(p) - N(n)},$$

where no information is defined by $N(n)$, medium grid cell-level information by $M(m)$, and perfect grid cell-level information across the landscape by $P(p)$.

2.4.3. Land Use/Land Cover Change Analysis. Following the classification of images (1987, 2002, and 2017) and prediction of the 2032 and 2047 situation, change statistics were computed through comparisons among the successive periods [13, 47, 71–74]. The conversion matrix of the past 30 years periods (1989–2017) was made to differentiate the changes of each land-use type [25, 34, 46, 72]. Furthermore, the percentage of change and rate of change was also

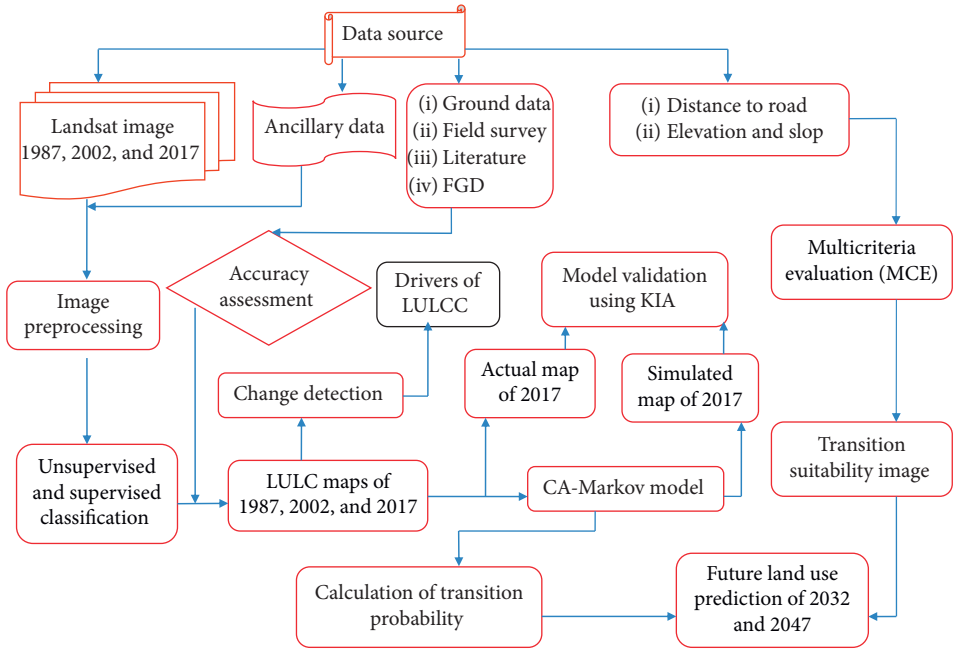

Figure 4: A schematic representation of the study adopted from Yirsawet al. [17].

computed using equations (3) and (4), respectively [13, 29, 72, 75].

$$\mathrm{RC}\left(\frac{\mathrm{ha}}{\mathrm{year}}\right) = \left(\frac{X-Y}{Z}\right),$$
$$\%\ \text{of change} = \left(\frac{X-Y}{Y}\right) * 100, \tag{6}$$

where RC is the rate of change, X is the area of LULC (ha) in the recent year, Y is the area of LULC (ha) in the past year, and Z is the time interval between X and Y in years.

2.5. Source of Data for LULC Change Drivers. A field survey was conducted to explore the socioeconomic data for showing the driver of LU/LC change based on the survey qualitative tools such as focus group discussion (FGD), key informant interview (KII), and household (HH) survey including field observation and document review. The ultimate purpose of the field survey was to collect quantitative data to help better understand, explain, and interpret the LULC change drivers [76–79] using semistructured questionnaires (close and open-ended). The data were generated from both primary and secondary sources. To do so, eight kebeles were purposively selected from two districts, Godere and Mengeshi, namely, Ashani, Baya, Fejeji, Newe, Akashi, Dunchaye, Gonchi, and Gelesha.

Household (HH) survey was conducted in eight kebeles of Godere and Mengeshi districts (four kebeles per district) from 10 March to May 2019. These kebeles were selected, based on the level of forest resources dependency communities. So, a total of 240 HHs were randomly selected and interviewed [80]. The questionnaires were envisioned to capture drivers of LULC changes perception, socioeconomic features of HHs, and related information [27]. Furthermore, FGD (head of agricultural office, natural resource expert, elders, women, model farmers, kebeles administrative chairman, and representatives of NGO working in the woredas) and KII (elders, leaders, and women) were conducted in all the selected kebeles for detailed analyses of LULC change drivers (Table 4). During the interviews and discussion, the main attentions were to get adequate information about the past and present trends of LULC change and identify the main driving causes of LULC change. The farmers were asked to explain what parts of the landscape were changed, describe the consequences of the changes in their livelihood, surroundings, and environment, and how their socioeconomic activity contributes to the land-use change.

2.5.1. Data Analysis of Household Survey. All the collected data from the respondents were subjected to descriptive statistics using SPPS version 20 software. Averages, percentages, and frequency descriptive statistics were used to describe HHs' socioeconomic characteristics, a ranking of LULC change drivers along with presenting in tables and graphs.

3. Results

3.1. Status of Land Use/Land Covers. Five LULC classes were identified in the study area for the specified period 1987–2017 (Figure 5). In 1987, the forestland accounts for 84.4% followed by farmland (13.2%), grassland (1.5%), and settlement and waterbody that cover 0.9% and 0.06% which shows minimal coverage of the Majang Forest Biosphere Reserve (Table 5). In 2002, forestland cover about 80.8% is followed by farmland (15.8%), while settlement, grassland, and waterbody accounted for 2%, 1.3%, and 0.06%,

Table 4: The number of participants in the HH, FGD, and KII in all kebeles.

Kebele	Total population	Total HH	Selected HH	Selected FGD	Selected KII
Ashani[1]	1,758	464	22	8	3
Baya[1]	1,565	422	20	8	3
Fejeji[1]	1,721	469	22	8	3
Newe[1]	1,358	360	17	8	3
Akashi[2]	6,170	1655	77	8	3
Dunchaye[2]	2,554	685	32	8	3
Gonchi[2]	1,556	428	20	8	3
Gelesha[2]	2,376	651	30	8	3
Total	19,561	5,134	240	64	24

Note. [1]Mengeshi and [2]Godere districts.

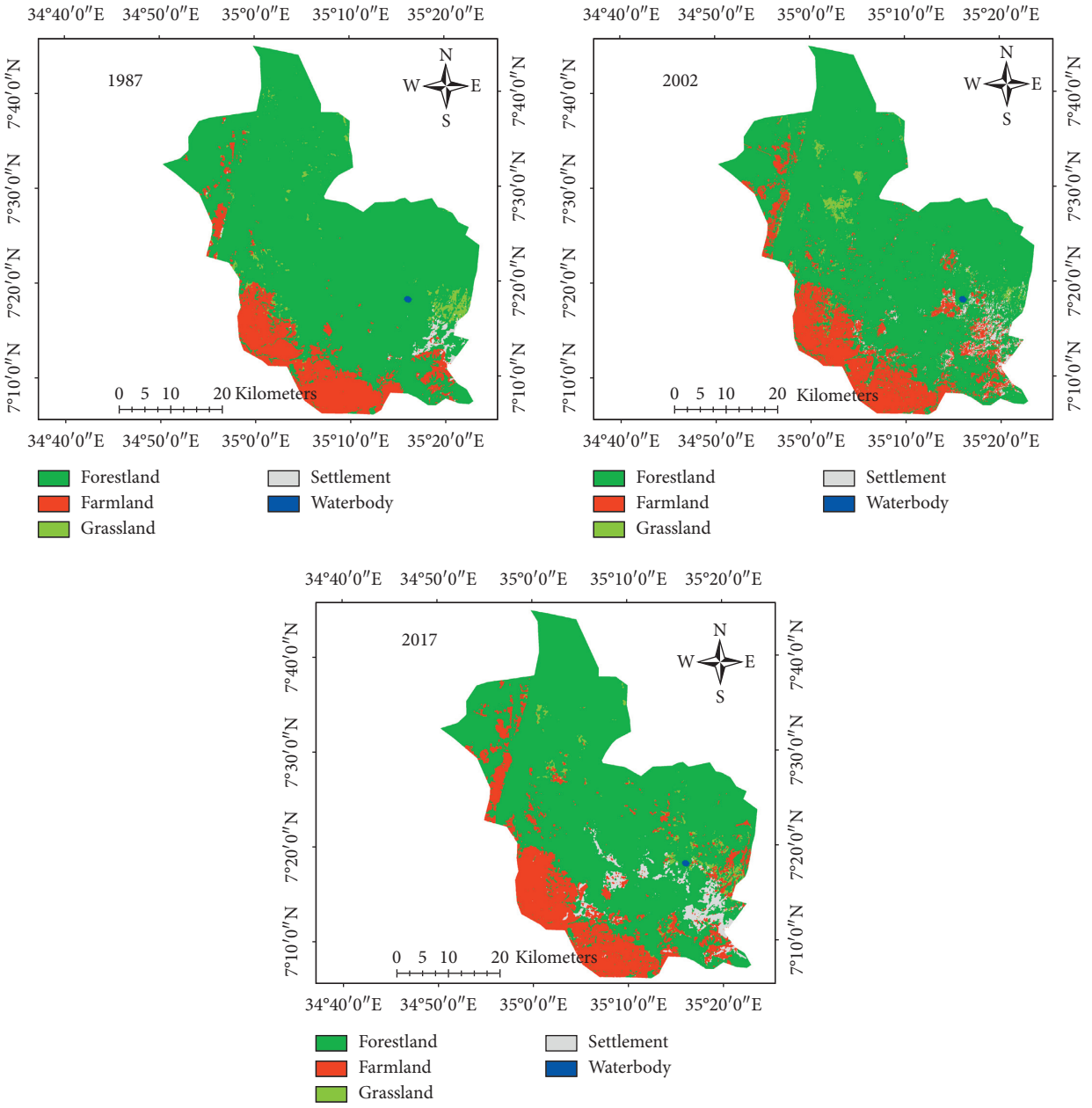

Figure 5: LULC of 1987, 2002, and 2017 in MFBR.

Table 5: Area of LULC class from 1987 to 2017 periods in MFBR.

Land use/land cover	1987		2002		2017	
	Area (ha)	Area (%)	Area (ha)	Area (%)	Area (ha)	Area (%)
Forestland	196761.6	84.4	188413.7	80.8	181504.9	77.8
Farmland	30781.8	13.2	36906.4	15.8	40554.8	17.4
Grassland	3509.2	1.5	3079.6	1.3	3192.2	1.4
Settlement	2050.7	0.9	4744.3	2.0	7866.2	3.4
Waterbody	141.0	0.06	141.0	0.06	141.0	0.06
Total	233254	100%	233254	100%	233254	100%

respectively. Forestland was declined to 77.8% in 2017, whereas farmland, settlement, and grassland increased by 17.4%, 3.4%, and 1.4%, respectively, but waterbody showed no significant changes with that of 1987 and 2002 (Table 5).

In all study periods, farmland and settlement significantly increase as the expense of forestland and grassland coverage, in which the forestland and grassland were decreased by 19,6761.6 to 18,1504.9 and 3,509.2 to 3,192.2 from 1987 to 2017 (Table 5).

3.2. LULC Conversions Analysis: 1987–2002 and 2002–2017. The land use/land cover change was performed by taking the initial year in 1985. Three LULC conversions were detected, i.e., between 1987 and 2002, 2002 and 2017, and 1987 and 2017. The land use/land cover conversions results revealed that a substantial loss and gains of LULC were inspected in the first (1987–2002), second (2002–2017), and third study periods. For instance, forestland was converted to other LULC classes during the first, second, and third study periods by about 556.5 ha (4.4%), 460.6 ha (3.8%), and 1017.1 ha (8.4%), respectively. Also, grassland was reduced by about 28.6 ha (13.6%) and 21.1 ha (9.5%) in the first and third study periods, respectively, while it increases by 7.5 ha 3.6% in the third study period. On the contrary, farmlands and settlements were expanded by 408.3 ha (16.6%), 243.2 ha (9%), and 651.5 ha (24.1%) and 179.6 ha (56.7%), 208.1 ha (39.8%), and 387.7 ha (73.9%) in the first, second, and third study periods, respectively, while in waterbody, only 0.3 ha converts to other land use in all study periods (Table 6).

The conversions of LU/LC from one class to another class were revealed in all study periods (Tables 7 and 8). The diagonals in the matrix from the tables are the persistence, while the off-diagonals are the conversions from one category to the others. Between 1987 and 2002 periods, 3732, 510, and 47 ha of farmland were converted from forestland, settlement, and grassland, respectively, while farmland gained from other LU/LC categories (Table 7). During this period, some areas of settlement were also converted from farmland (519 ha), forestland (458 ha), and grassland (10 ha). Although, about 2764 ha, 510 ha, and 402 ha of the settlement were also converted to forestland, farmland, and grassland, respectively. Gains and losses in forestland and grassland were also taken place in all study periods (Table 7).

Between, 2002 and 2017 periods, 4312 ha, 1773 ha, 1114 ha, and 6 ha of forestland were also converted to farmland, grassland, settlement, and waterbody, respectively. Similarly, forestland, grassland, and settlement were also gained from other LU/LC categories (Table 8). In these periods, a significant area of farmland was converted from forestland (4312 ha), settlement (2418), and grassland (206 ha). In reverse, there was also a considerable conversion of farmland to other categories. A significant amount of gains and losses in the settlement has also occurred in these periods (Table 8).

3.3. Future Land Use/Land Cover Change

3.3.1. Actual and Simulated LULC of MFBR for 2017. Actual and simulated LULC of MFBR was developed for the year 2017. Accordingly, the actual and simulated maps of the year 2017 depicted soundly similarity in waterbody cover, while slight differences were depicted in other LULC classes (Figure 6). The area coverage of the two maps showed that all land use/land cover classes have the best range of agreement with a rate of difference lower than 10% (Table 9).

Regarding model validation, kappa index of agreement (K_{IA}) comparison was made between the actual and simulated LULC maps of 2017. The validation of the model or K_{IA} statistics (Table 8) and the actual and predicted LULC change of the 2017 period (Table 10) result showed a good similarity between the actual and predicted maps of 2017. The overall kappa value is 87.3% which represents a strong agreement between the two map categories. Such a validation process was evaluating the agreement of the two maps (predicted and actual) in terms of the number of pixels in each LULU class and in term of their location of the pixels.

3.3.2. Predicted Land/Use Land Cover. The projected land use/land cover types of 2032 and 2047 were computed using the CA-Markov model as presented in Figure 7, whilst their area are given in Table 11. The area of forestland and grassland decreased from 72.4 in 2032 to 66.5 in 2047 and 1.2 in 2032 to 0.8 in 2047, respectively. A continuous increase in farmland and settlement will be observed in 2032 (21.5%) to 2047 (26.3) and 2032 (4.9) to 2047 (6.4), respectively. On the other hand, waterbody will depict almost a constant percentage in 2032 (0.05%) to 2047 (0.05%), while it will be decreased in area coverage from 135 ha to 126 ha in 2032 and 2047, respectively. In addition, as compared to LULC 2017–2047 farmland and settlement increased by 8.9% and 3%, respectively, while forestland and grassland decreased by 11.3% and 0.6%, respectively. The expansion of farmland and settlement is expected to increase at the expense of forestland and grassland.

Table 6: Percentage and rate of changes occurred in MFBR from 1987 to 2017 periods.

LU/LC	PC			RC (ha/year)		
	1987–2002	2002–2017	1987–2017	1987–2002	2002–2017	1987–2017
Forestland	−4.4	−3.8	−8.4	−556.5	−460.6	−1017.1
Farmland	16.6	9.0	24.1	408.3	243.2	651.5
Grassland	−13.6	3.6	−9.5	−28.6	7.5	−21.1
Settlement	56.7	39.8	73.9	179.6	208.1	387.7
Waterbody	0.0	0.0	0.0	0.0	−0.3	−0.3

Note. MFBR = Majang Forest Biosphere Reserve, PC = percentage of change, and RC = rate of change.

Table 7: Transition area matrix (ha) between 1987 and 2002 in MFBR.

1987	2002					
	Forestland	Farmland	Grassland	Settlement	Waterbody	Total
Forestland	182378	3732	1800	458	3	188372
Farmland	9093	26486	786	519	0	36884
Grassland	2502	47	520	10	0	3079
Settlement	2764	510	402	1062	0	4739
Waterbody	3	0	0	0	138	141
Total	196740	30775	3509	2049	141	233254

Table 8: Transition area matrix (ha) between 2002 and 2017 in MFBR.

2002	2017					
	Forestland	Farmland	Grassland	Settlement	Waterbody	Total
Forestland	174287	4312	1773	1114	6	181492
Farmland	8384	29956	829	1375	0	40544
Grassland	2237	206	455	293	0	3191
Settlement	3467	2418	21	1958	0	7864
Waterbody	2	0	0	0	134	136
Total	188377	36892	3078	4740	140	233254

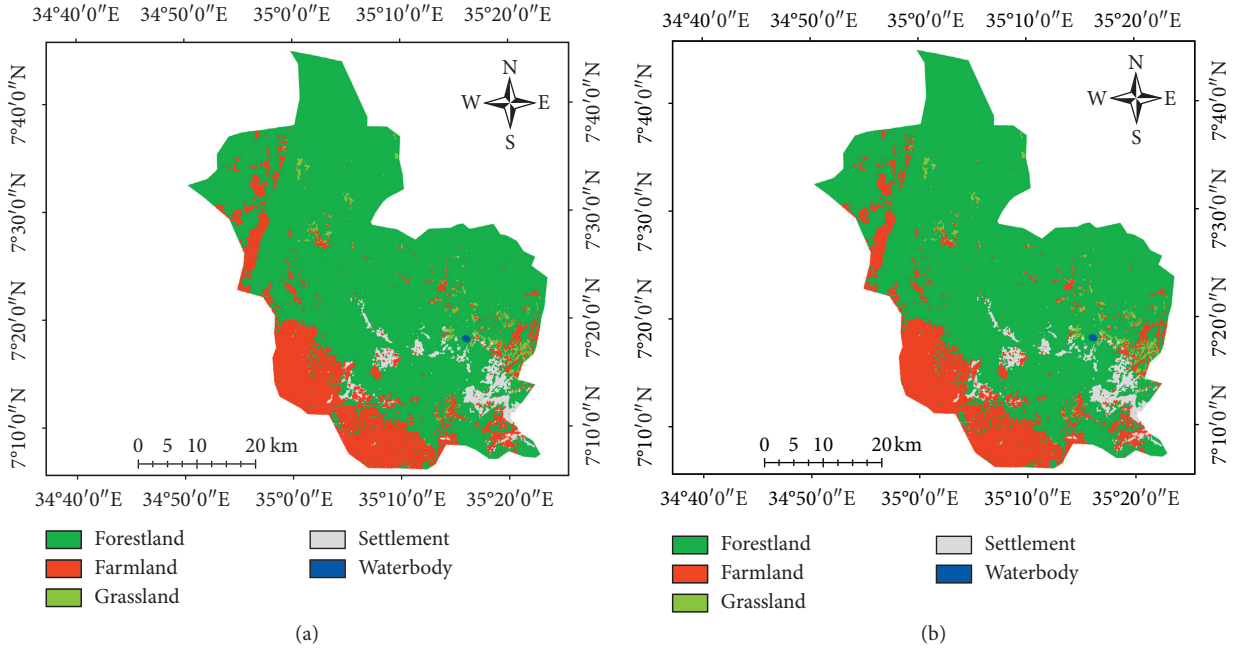

Figure 6: The actual (a) and simulated (b) LULC maps of MFBR for 2017.

Table 9: Statistical validation of the CA-Markov chain model.

Statistics	Value (%)
$K_{standard}$	85.3
K_{no}	81.2
$K_{location}$	81.4
$K_{locationstrata}$	80.8
Overall K	87.3

Table 10: Comparison of actual and simulated LULC changes in 2017.

LULC class	Actual (2017)		Simulated (2017)		Changes	
	Area (ha)	Area (%)	Area (ha)	Area (%)	RC (ha)	PC
Forestland	181504.9	77.8	180980.7	77.6	−524.2	−0.2
Farmland	40554.8	17.4	41014.7	17.5	459.9	0.2
Grassland	3192.2	1.4	3002.5	1.3	−189.7	−0.1
Settlement	7866.2	3.4	8120.6	3.5	254.4	0.1
Waterbody	141	0.06	141	0.06	−1	0
Total	233254	100%	233254	100		

Note. PC = percentage of change, RC = rate of change.

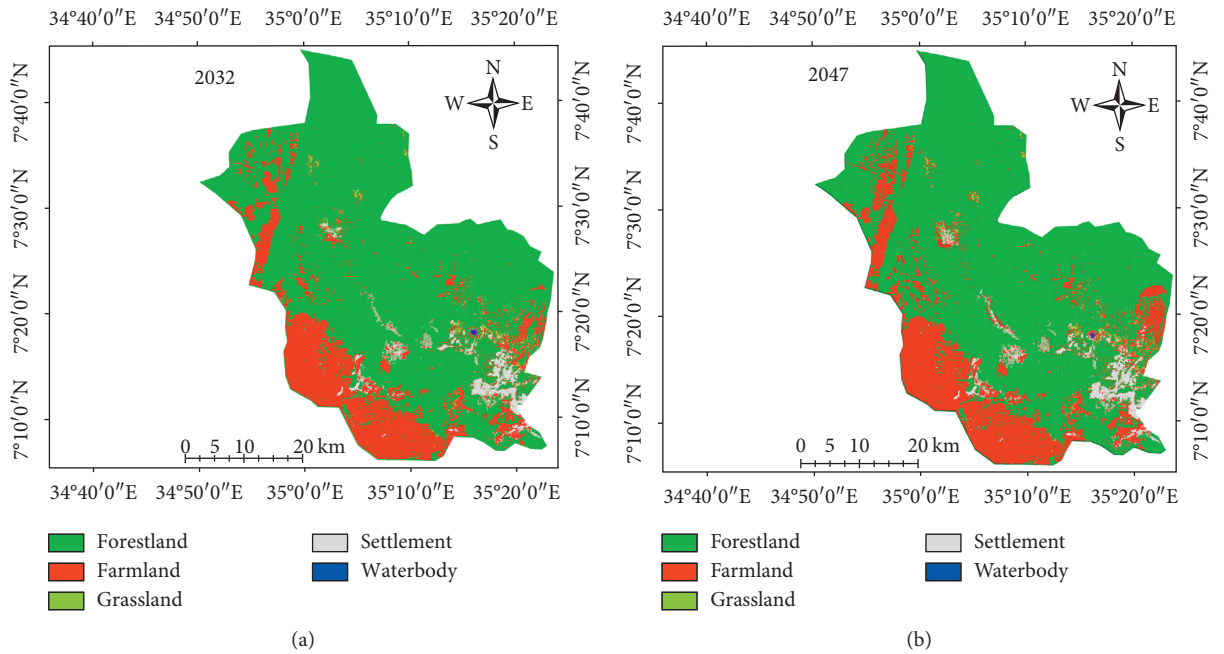

Figure 7: The 2032 and 2047 predicted LULC of MFBR.

Table 11: LULC area change (ha) from 2017 to 2047of MFBR.

LULC class	2017		2032		2047		(2017–2047)	
	Area	%	Area	%	Area	%	RC (ha)	PC
Forestland	181504.9	77.8	168800.7	72.4	155020.7	66.5	−26484.2	11.3
Farmland	40554.8	17.4	50151.8	21.5	61476.8	26.3	20922	8.9
Grassland	3192.2	1.4	2740.2	1.2	1788.5	0.8	−1403.7	0.6
Settlement	7866.2	3.4	11426.2	4.9	14840.2	6.4	6974	3
Waterbody	141	0.06	135	0.05	126	0.05	−15	0.01
Total	233254	100%	233254	100%	233254	100%		

Note. MFBR = Majang Forest Biosphere Reserve, PC = percentage of change, and RC = rate of change.

In addition, as the result shows in Figure 8, a reduction of forestland cover from 84.4%, 80.78%, 77.8%, 72.4%, and 66.5%; grassland from 1.5%, 1.3%, 1.4%, 1.2%, and 0.8%; and waterbody from 0.06% to 0.05% were examined through the 1987–2047 study period, respectively. While farmland and settlement increased from13.2%, 15.82%, 17.4%, 21.5%, and 26.3% and 0.88%, 2.03%, 3.37%, 4.9%, and 6.4% at the expense of forestland through the 1987–2047 study period (Table 11).

The conversion of LU/LC classes also has been taken place between 2017 and 2045 predicted periods (Table 11). For example, between predicted periods 2017 and 2047 of forestland, grassland, and waterbody were reverted to farmland and settlement during the predicted periods by 26484.2 ha (11.3%), 1403.7 ha (0.6%), and 15 ha (0.01%), respectively. On the contrary, farmlands and settlements were expanded by 20922 ha (8.9%) and 6974 ha (3%) in the predicted periods, respectively.

3.4. Drivers of LULC Changes Based on Respondents View. Based on the respondents' survey results and field observation, multiple factors contributed to LULC changes in the study area. However, there was the difference in each of the factors to which the local community observed drivers of LULC changes. The survey and field observation showed that forestland and grassland were converted to farmland and settlements which are similar to LU/LC result. Regarding identification of driving factors of LULC changes, out of nine LULC change driving factors, the top four driving factors mentioned by the respondents in the study area were agriculture expansion (15.6%), human population growth (15.5%), wood extraction (14.6%), and risk of fire (14%), respectively (Table 12).

The population growth was perceived as the second driving factor causing LULC change. Based on 2007 Population Census of Ethiopia, the total population of Majang Zone was 59,248 [81], and the population was estimated to be 77,022 in 2014 and 82,268 in 2017. Thus, increment of the population between two census periods (2007 and 2014) varied from 3% in Akashi kebele to 27% in Ashani and Gonchi kebeles (Table 13). The increase of population in the study area demands land for agriculture, grazing land firewood, and settlement which could influence future land use/land cover.

Also, results from FGD and KII confirmed that population growth coupled with "resettlement of 1984/5" and "villagization of 2011" policies resulted in an extraexpansion of settlement and agricultural land at the expanses of forest and grassland. Besides, the "Land to Tiller" of 1970s policy including the absence of proper land use plans played a role in conversion of forest and grassland to settlement and farmland in the study area.

Based on the secondary data, the most recent phenomenon causing widespread forest destruction in the study area was an agricultural investment that began during 2003. About 19,165.83 ha of land were provided to investors or companies. For instance, Green Coffee, Verdanta, Marekose, and Afero-Tseyone companies were provided 6500 ha, 3012 ha, 3000 ha, and 2000 ha of land, respectively, in the study area (Table 14). It is inspected that land transfer to investors is a common phenomenon that aggravates land use/land cover changes. Also, the key informants reported that "land transfer to investors" puts strong pressure on the remaining forests to convert other LULC in the study area.

4. Discussion

4.1. Land Use/Land Cover Change. Computation of remotely sensed data is the well-established field of study that aids in articulating changes and patterns of land use/land covers in temporal and spatial aspects. Land use/land cover change analysis of the study area was run, and maps were generated for the last three decades, 1987–2017. The overall accuracies were attained by Landsat TM (85.4%), ETM+ (86%), and OLI-TIRS (87.3%) for the years 1987, 2002, and 2017 (Table 3). The values overall accuracy and kappa values above 80% indicate that the classification performance is satisfactory [82]. The results of this study are more or less related to other local studies such as Landsat TM (86.9%), ETM+ (85.8%), and OLI-TIRS (88.8%); Landsat MSS (83.1%), TM (85.8%), and ETM+ (88.7%); and Landsat MSS (85.5%), ETM+ (83.15%), and ETM+ (87.73%) [30, 41].

A total of five LULC types were identified in the study area in all study periods (1987–2017) (Figure 5); a forestland accounted for the largest proportion of farmland, grassland, settlement, and waterbody. Forestland and grassland were decreased and mainly transformed into farmland and settlement in all study periods (Table 6). This is possibly due to agricultural expansion as a result of human population increment in the study site. The finding of this research is consistent with other studies carried out in different parts of the country, for instance, Zeleke and Humi [21] in Dembecha area of northwest Ethiopia stated that 99% of the forest cover was transformed into farmland between 1957 and 1995. Similarly, Kindu et al. [8] in Munessa-Shashemene landscape of the Ethiopian highlands stated that almost 66.2% of woodland is converted to farmland. Many other local LULC studies also indicated similar trends [13, 29, 83, 84]. Also, a study in Baro river basin in southwestern Ethiopia showed the conversion of forest land to nonforestland between 1984 and 2010 mainly by the expansion of farmland and settlement [85]. In contrary, forestland was increased by 27% in Chemoga watershed in the Blue Nile, which was the result of the community afforestation program in a degraded hilly area in the watershed [86]. Moreover, land use/land cover conversions results revealed that a substantial loss and gains of LULC were inspected in the first and second study periods. For instance, forestland was converted to other LULC classes, while farmlands and settlements were gained from forestland and grassland during the first and second study periods (Tables 7 and 8). These changes may affect the habitat of key species in the area [87, 88]. Destruction of habitats and decrease in their sizes may lead to restriction and decline of species ecological niches.

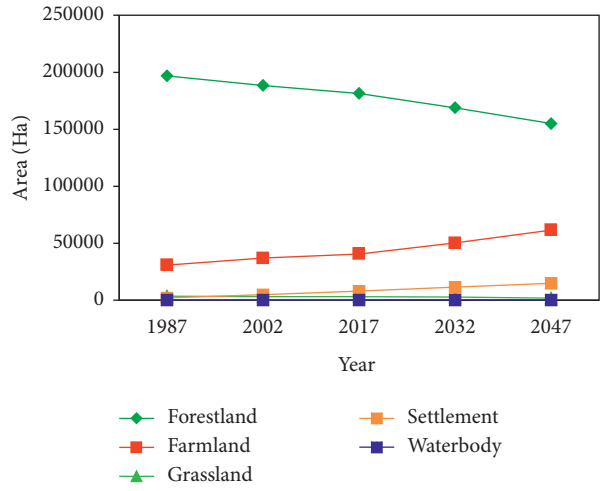

Figure 8: Trends of LULCC from 1985 to 2045 in MFBR.

Table 12: Land use/land cover change key drivers and ranking.

Drivers of LULC changes	Percentage (%)	Rank
Agriculture expansion	15.6	1
Population growth	15.5	2
Wood extraction (for charcoal, fuel wood, and construction)	14.6	3
Fire	14.0	4
Expansion of settlement	11.6	5
Infrastructure development	10.6	6
Lack of forest policies and laws	7.4	7
Limited capacities of the forest sector	6.4	8
Absence of land use planning	4.3	9

Table 13: Population number and growth rate in the sample kebeles of Majang Zone.

Name of kebele	2007	2014 (E)	Growth between 2007 and 2014	Change between 2007 and 2014 (%)	Growth rate (%) between 2007 and 2014	Doubling time after 2014
Ashani[1]	388	1758	1370	353	27	3
Baya[1]	381	1565	1184	311	24	3
Fejeji[1]	446	1721	1275	286	22	3
Newe[1]	307	1358	1051	342	26	3
Akashi[2]	4,269	6170	1901	45	3	20
Dunchaye[2]	1,536	2554	1018	66	5	14
Gelesha[2]	1,249	2376	1127	90	7	10
Gonchi[2]	345	1556	1211	351	27	3

Note. [1]Mengeshi and [2]Godere district. E, estimated.

4.2. Future Land Use/Land Cover Change. The CA-Markov chain is a stochastic procedures model that pronounces the possibility of change from one land use/land cover class into another land use/land cover class using a transition probability matrix [89, 90]. The most suitable model for predicting LULC change is the CA-Markov chain model [66]. This model is appropriate if the changes and procedures in a given landscape are challenging to describe. Regarding to model validation of this study, kappa index of agreement (KIA) comparison was made between the actual and simulated LULC map of 2017. The validation of the model or KIA statistics (Table 9) result showed a good similarity between the actual and predicted map of 2017. The actual and simulated maps for year 2017 were depicted reasonably similar for waterbody, while for the other LULC classes, there were almost slight differences between simulated and actual maps. However, considering the overall K_{IA} was a high level of agreement standards, and they were between 75% ≤kappa <100 [60, 70], which indicates the good agreement between the actual and simulated LULC maps [13, 48, 57, 71]. Therefore, the CA-Markov model is an effective tool and is reliable to simulate, predict, and analyse different changes of LULC in 2032 and 2047. With comparable kinds of agreement and disagreement result, [91]

Table 14: Leased land for private companies investment in Majang Zone.

Company name	Area (ha)	Year of licensed	Lease period (years)
Green Coffee	6500	2015	50
Verdanta	3012	2015	50
Marekose	3000	2015	50
Afero-Tseyone	2000	2015	50
G/Medihen	1400	2014	50
Majang Agro-Industry	1000	2015	50
Shake Agro-Industry	763	2015	50
Ebdayetaye	488	2013	50
Tekalign	355	2015	50
Siraje Negaw	362	2003	50
Adenew Angelo	189.83	2006	50
Total	19,165.83		

showed that the CA-Markov model might be taken as an effective model in prediction of LULC changes. The prediction of 2032 and 2047 result showed reduction of forestland, grassland, and waterbody cover, while farmland and settlement were increased at the expense of forestland and grassland in the predicted period (Figure 8), which is consistence with other findings [13, 17, 92]. The area extent of the forestland cover is likely to be taken over by farmland and settlement in the predicted period (Table 10), which may be due to future anthropogenic activities (farmland and settlement expansion) coupled with population increment in the area. These prediction results might be used as a guide for conservation planning in the area, assisting decision-makers to improve land use management plans to balance development and conservation.

4.3. Drivers of Land Use/Land Cover Changes. In general, LULC change is the result of the comprehensive influences of so many complex and various factors [93, 94]. Previous studies have revealed that on a global scale, human-driven land use/land cover change for most of the changes of land surface. However, the key driving factors vary according to the nature and magnitude of the area [95]. In this study, we analysed multiple driving factors contributed to LULC changes in the study area. Accordingly, the most important drivers of LULC change in the study area were agriculture expansion, population growth, wood extraction, and charcoal and fire (Table 12). Most importantly, agricultural expansion and population growth were more experienced as compared to other driving factors. This is similar with other finding reports in Ethiopia [13, 27, 35, 36]. Moreover, the driver plays a role in intensive loss of forestland to other land uses in the study area due to brutal drought and famine that affects the country, and the government implemented resettlement and villagization in the study area to combat the impacts of drought, which was aimed to move farmers from northern into southwestern parts of the country [96]. For instance, during the 1980s, at Gambella region (Godere, Zuria and Abobo) were settled about 11,234 households with land 15,600 ha, respectively [97]. FGD and KII also confirmed that population growth coupled with resettlement (1984) and villagization (2010) in the study area that resulted in further expansion of agricultural land as expanses of forestland which was the main driving force of LULC change in the area. For instance, increased population number is observed in the sample kebele both in national count in 2007 and 2014 which was evident largely through the expansion of farmlands at the expense of forestland cover [98, 99]. Likewise, a significant loss of the grasslands to other land use was observed in the area as a result of the expansion of agriculture and rapid population growth. Similar results were reported in different parts of Ethiopia [13, 83, 96, 100].

5. Conclusion

Land use/land cover change (LULC) analyses are crucial for a well-informed decision-making regarding proper land uses planning policy. This study identified five LULC classes such as forestland, farmland, grassland, settlement, and waterbody in the study area, for the study periods of 1987–2017. Based on the LULC changes, farmland and settlement increased while forestland and grassland were reduced in the study period of time (1987–2017). A broad-spectrum trend was inspected as increment of farmland and settlement areas; meanwhile, shrinkage of forestland, grassland, and waterbody will continue in the near future, 2032–2047. Eventually, based on the respondents ranking, the main drivers of LULC changes were identified as agricultural expansion, human population growth, shifting cultivation, fuel wood extraction, and fire risk. Moreover, results from focus group discussion (FGD) also confirmed that population growth coupled with resettlement and villagization have resulted in further expansion of agricultural land as expanses of forestland. Generally, substantial LULC changes were observed and most likely continued onward until the specified future period of this study. Hence, a rational land use plan should be proposed in order to sustain livelihoods of local communities, resources of MFBR, and the environment. Likewise, the predicted model applied in this study delivers basic information that the planner should consider extensive driving factors of physical, social, and economic associated with the complex use of land. Moreover, this study also proposes a further study on the impacts brought by LULC change, specifically climate and watershed hydrology; meanwhile, this study addressed only LULC change, driving forces behind the changes, and future prediction.

Data Availability

The data used to support the findings of this study are included within this article without restriction and in its supporting information file.

Conflicts of Interest

The authors declare that there are no conflicts of interest.

Acknowledgments

The authors would like to thank Center for Environmental Science, Addis Ababa University, for their contribution. This study was funded by Addis Ababa University.

Supplementary Materials

S1 Table. Attributes of sampled households in the study area ($N = 240$), exploring overviews of respondent profiles, specifically socioeconomic attributes such as family size, occupation, size of landholdings, and education status are essential in terms of identifying and understanding driving factors of land use/land cover changes in the study area. Henceforth, some of the relevant attributes are summarized in this supporting table. S2 Table. Mean rainfall and temperature in the study area station which is used in suitability map preparation to predict the future LULC (MAR, mean annual rainfall; MAT, mean annual temperature). S3 and S4 Tables. Mean monthly mean temperature and rainfall (30 year mean) for climate description in Tinishu Meti and Tinishu Ermichi. (*Supplementary Materials*)

References

[1] B. L. Turner, D. Skole, S. Sanderson, G. Fischer, L. Fresco, and R. Leemans, *Land-use and Land-Cover Change: Science/research Plan*, IGBP, Stockholm, 1995.

[2] H. A. Kaul and I. Sopan, "Land use land cover classification and change detection using high resolution temporal satellite data," *Journal of Environment*, vol. 1, no. 4, pp. 146–152, 2012.

[3] W. B. Meyer, W. B. Meyer, and I. B. L. Turner, *Changes in Land Use and Land Cover: A Global Perspective*, Vol. 4, Cambridge University Press, Cambridge, UK, 1994.

[4] B. M. Sleeter, T. L. Sohl, T. R. Loveland et al., "Land-cover change in the conterminous United States from 1973 to 2000," *Global Environmental Change*, vol. 23, no. 4, pp. 733–748, 2013.

[5] M. Niedertscheider, T. Kuemmerle, D. Müller, and K.-H. Erb, "Exploring the effects of drastic institutional and socio-economic changes on land system dynamics in Germany between 1883 and 2007," *Global Environmental Change*, vol. 28, pp. 98–108, 2014.

[6] A. S. Belward and J. O. Skøien, "Who launched what, when and why; trends in global land-cover observation capacity from civilian earth observation satellites," *ISPRS Journal of Photogrammetry and Remote Sensing*, vol. 103, pp. 115–128, 2015.

[7] S. E. Taelman, T. Schaubroeck, S. De Meester, L. Boone, and J. Dewulf, "Accounting for land use in life cycle assessment: the value of NPP as a proxy indicator to assess land use impacts on ecosystems," *Science of the Total Environment*, vol. 550, pp. 143–156, 2016.

[8] M. Kindu, T. Schneider, D. Teketay, and T. Knoke, "Land use/land cover change analysis using object-based classification approach in Munessa-Shashemene landscape of the Ethiopian highlands," *Remote Sensing*, vol. 5, no. 5, pp. 2411–2435, 2013.

[9] S. D. Dayamba, H. Djoudi, M. Zida, L. Sawadogo, and L. Verchot, "Biodiversity and carbon stocks in different land use types in the Sudanian Zone of Burkina Faso, West Africa," *Agriculture, Ecosystems & Environment*, vol. 216, pp. 61–72, 2016.

[10] A. Alam, M. S. Bhat, and M. Maheen, "Using landsat satellite data for assessing the land use and land cover change in Kashmir valley," *GeoJournal*, vol. 85, pp. 1529–1543, 2019.

[11] A. Javed, S. Jamal, and M. Y. Khandey, "Climate change induced land degradation and socio-economic deterioration: a remote sensing and gis based case study from Rajasthan, India," *Journal of Geographic Information System*, vol. 4, no. 3, 2012.

[12] F. J. Gallego, "Remote sensing and land cover area estimation," *International Journal of Remote Sensing*, vol. 25, no. 15, pp. 3019–3047, 2004.

[13] T. Gashaw, T. Tulu, M. Argaw, and A. W. Worqlul, "Evaluation and prediction of land use/land cover changes in the Andassa watershed, Blue Nile Basin, Ethiopia," *Environmental Systems Research*, vol. 6, no. 1, p. 17, 2017.

[14] C. Hyandye and L. W. Martz, "A Markovian and cellular automata land-use change predictive model of the Usangu Catchment," *International Journal of Remote Sensing*, vol. 38, no. 1, pp. 64–81, 2017.

[15] M. Kindu, T. Schneider, D. Teketay, and T. Knoke, "Changes of ecosystem service values in response to land use/land cover dynamics in Munessa-Shashemene landscape of the Ethiopian highlands," *Science of the Total Environment*, vol. 547, pp. 137–147, 2016.

[16] E. Zadbagher, K. Becek, and S. Berberoglu, "Modeling land use/land cover change using remote sensing and geographic information systems: case study of the Seyhan Basin, Turkey," *Environmental Monitoring and Assessment*, vol. 190, no. 8, p. 494, 2018.

[17] E. Yirsaw, W. Wu, X. Shi, H. Temesgen, and B. Bekele, "Land use/land cover change modeling and the prediction of subsequent changes in ecosystem service values in a coastal area of China, the Su-Xi-Chang Region," *Sustainability*, vol. 9, no. 7, p. 1204, 2017.

[18] S. Roy, K. Farzana, M. Papia, and M. Hasan, "Monitoring and prediction of land use/land cover change using the integration of Markov chain model and cellular automation in the southeastern tertiary hilly area of Bangladesh," *International Journal of Sciences: Basic and Applied Research*, vol. 24, pp. 125–148, 2015.

[19] L. Sang, C. Zhang, J. Yang, D. Zhu, and W. Yun, "Simulation of land use spatial pattern of towns and villages based on CA–Markov model," *Mathematical and Computer Modelling*, vol. 54, no. 3-4, pp. 938–943, 2011.

[20] B. M. Sleeter, T. L. Sohl, M. A. Bouchard et al., "Scenarios of land use and land cover change in the conterminous United States: utilizing the special report on emission scenarios at ecoregional scales," *Global Environmental Change*, vol. 22, no. 4, pp. 896–914, 2012.

[21] G. Zeleke and H. Hurni, "Implications of land use and land cover dynamics for mountain resource degradation in the Northwestern Ethiopian highlands," *Mountain Research and Development*, vol. 21, no. 2, pp. 184–191, 2001.

[22] B. Tegene, "Land-cover/land-use changes in the derekolli catchment of the South Welo zone of Amhara region, Ethiopia," *Eastern Africa Social Science Research Review*, vol. 18, no. 1, pp. 1–20, 2002.

[23] A. Amsalu, L. Stroosnijder, and J. d. Graaff, "Long-term dynamics in land resource use and the driving forces in the Beressa watershed, highlands of Ethiopia," *Journal of Environmental Management*, vol. 83, no. 4, pp. 448–459, 2007.

[24] G. Dessie and J. Kleman, "Pattern and magnitude of deforestation in the South central rift valley region of Ethiopia," *Mountain Research and Development*, vol. 27, no. 2, pp. 162–168, 2007.

[25] T. H. M. Rientjes, A. T. Haile, E. Kebede, C. M. M. Mannaerts, E. Habib, and T. S. Steenhuis, "Changes in land cover, rainfall and stream flow in Upper Gilgel Abbay catchment, Blue Nile basin-Ethiopia," *Hydrology and Earth System Sciences*, vol. 15, no. 6, pp. 1979–1989, 2011.

[26] T. G. Gebremicael, Y. A. Mohamed, G. D. Betrie, P. van der Zaag, and E. Teferi, "Trend analysis of runoff and sediment fluxes in the Upper Blue Nile basin: a combined analysis of statistical tests, physically-based models and landuse maps," *Journal of Hydrology*, vol. 482, pp. 57–68, 2013.

[27] M. Kindu, T. Schneider, D. Teketay, and T. Knoke, "Drivers of land use/land cover changes in Munessa-Shashemene landscape of the south-central highlands of Ethiopia," *Environmental Monitoring and Assessment*, vol. 187, no. 7, p. 452, 2015.

[28] M. Kindu, T. Schneider, M. Döllerer, D. Teketay, and T. Knoke, "Scenario modelling of land use/land cover changes in Munessa-Shashemene landscape of the Ethiopian highlands," *Science of the Total Environment*, vol. 622-623, pp. 534–546, 2018.

[29] T. Gashaw, A. Bantider, and A. Mahari, "Evaluations of land use/land cover changes and land degradation in Dera district, Ethiopia: GIS and remote sensing based analysis," *International Journal of Scientific Research in Environmental Sciences*, vol. 2, no. 6, p. 199, 2014.

[30] T. Gashaw, T. Tulu, M. Argaw, A. W. Worqlul, T. Tolessa, and M. Kindu, "Estimating the impacts of land use/land cover changes on ecosystem service values: the case of the Andassa watershed in the Upper Blue Nile basin of Ethiopia," *Ecosystem Services*, vol. 31, pp. 219–228, 2018.

[31] M. Minta, K. Kibret, P. Thorne, T. Nigussie, and L. Nigatu, "Land use and land cover dynamics in Dendi-Jeldu hilly-mountainous areas in the central Ethiopian highlands," *Geoderma*, vol. 314, pp. 27–36, 2018.

[32] M. Woldetsadik, "Population growth and environmental recovery: more people, more trees, lesson learned from West Gurageland," *Ethiopian Journal of the Social Sciences and Humanities*, vol. 1, no. 1, pp. 1–33, 2003.

[33] R. N. Munro, J. Deckers, M. Haile, A. T. Grove, J. Poesen, and J. Nyssen, "Soil landscapes, land cover change and erosion features of the Central Plateau region of Tigrai, Ethiopia: photo-monitoring with an interval of 30 years," *Catena*, vol. 75, no. 1, pp. 55–64, 2008.

[34] D. Tsegaye, S. R. Moe, P. Vedled, and E. Aynekulu, "Land-use/cover dynamics in Northern Afar rangelands, Ethiopia," *Agriculture, Ecosystems & Environment*, vol. 139, no. 1-2, pp. 174–180, 2010.

[35] M. A. Wubie, M. Assen, and M. D. Nicolau, "Patterns, causes and consequences of land use/cover dynamics in the Gumara watershed of lake Tana basin, Northwestern Ethiopia," *Environmental Systems Research*, vol. 5, no. 1, p. 8, 2016.

[36] A. WoldeYohannes, M. Cotter, G. Kelboro, and W. Dessalegn, "Land use and land cover changes and their effects on the landscape of Abaya-Chamo Basin, Southern Ethiopia," *Land*, vol. 7, no. 1, p. 2, 2018.

[37] E. Garedew, M. Sandewall, U. Söderberg, and B. M. Campbell, "Land-use and land-cover dynamics in the central rift valley of Ethiopia," *Environmental Management*, vol. 44, no. 4, pp. 683–694, 2009.

[38] J. M. Olson, G. Alagarswamy, J. A. Andresen et al., "Integrating diverse methods to understand climate-land interactions in East Africa," *Geoforum*, vol. 39, no. 2, pp. 898–911, 2008.

[39] R. Mahmood, R. A. Pielke, K. G. Hubbard et al., "Impacts of land use/land cover change on climate and future research priorities," *Bulletin of the American Meteorological Society*, vol. 91, no. 1, pp. 37–46, 2010.

[40] T. Paz-Kagan, M. Shachak, E. Zaady, and A. Karnieli, "Evaluation of ecosystem responses to land-use change using soil quality and primary productivity in a semi-arid area, Israel," *Agriculture, Ecosystems & Environment*, vol. 193, pp. 9–24, 2014.

[41] B. Fu, L. Chen, K. Ma, H. Zhou, and J. Wang, "The relationships between land use and soil conditions in the hilly area of the loess plateau in northern Shaanxi, China," *Catena*, vol. 39, no. 1, pp. 69–78, 2000.

[42] R. A. Pielke, A. Pitman, D. Niyogi et al., "Land use/land cover changes and climate: modeling analysis and observational evidence," *Wiley Interdisciplinary Reviews: Climate Change*, vol. 2, no. 6, pp. 828–850, 2011.

[43] A. I. Lyapustin, Y. Wang, I. Laszlo et al., "Multi-angle implementation of atmospheric correction for MODIS (MAIAC): 3. Atmospheric correction," *Remote Sensing of Environment*, vol. 127, pp. 385–393, 2012.

[44] J. Feranec, G. Hazeu, S. Christensen, and G. Jaffrain, "Corine land cover change detection in Europe (case studies of the Netherlands and Slovakia)," *Land Use Policy*, vol. 24, no. 1, pp. 234–247, 2007.

[45] K. G. MacDicken, "Global forest resources assessment 2015: what, why and how?" *Forest Ecology and Management*, vol. 352, pp. 3–8, 2015.

[46] E. Teferi, S. Uhlenbrook, W. Bewket, J. Wenninger, and B. Simane, "The use of remote sensing to quantify wetland loss in the Choke Mountain range, Upper Blue Nile basin, Ethiopia," *Hydrology and Earth System Sciences*, vol. 14, no. 12, pp. 2415–2428, 2010.

[47] J. J. Schulz, L. Cayuela, C. Echeverria, J. Salas, and J. M. Rey Benayas, "Monitoring land cover change of the dryland forest landscape of Central Chile (1975–2008)," *Applied Geography*, vol. 30, no. 3, pp. 436–447, 2010.

[48] V. N. Mishra, P. K. Rai, and K. Mohan, "Prediction of land use changes based on land change modeler (lcm) using remote sensing: a case study of Muzaffarpur (Bihar), India," *Journal of the Geographical Institute'Jovan Cvijic'SASA*, vol. 64, no. 1, 2014.

[49] R. Regmi, S. Saha, and M. Balla, "Geospatial analysis of land use land cover change modeling at Phewa lake watershed of Nepal by using cellular automata markov model," *International Journal of Current Engineering and Technology*, vol. 4, pp. 2617–2627, 2014.

[50] Q. Weng, "Land use change analysis in the Zhujiang delta of China using satellite remote sensing, GIS and stochastic modelling," *Journal of Environmental Management*, vol. 64, no. 3, pp. 273–284, 2002.

[51] X. Yang, X.-Q. Zheng, and R. Chen, "A land use change model: integrating landscape pattern indexes and Markov-CA," *Ecological Modelling*, vol. 283, pp. 1–7, 2014.

[52] P. Fitzsimmons and R. Getoor, "Homogeneous random measures and strongly supermedian kernels of a Markov process," *Electronic Journal of Probability*, vol. 8, 2003.

[53] P. Ghosh, A. Mukhopadhyay, A. Chanda et al., "Application of cellular automata and Markov-chain model in geospatial

environmental modeling-a review," *Remote Sensing Applications: Society and Environment*, vol. 5, pp. 64–77, 2017.
[54] A. Veldkamp and E. F. Lambin, *Predicting Land-Use Change*, Elsevier, Amsterdam, Netherlands, 2001.
[55] N. Q. Omar, M. S. S. Ahamad, W. M. A. Wan Hussin, N. Samat, and S. Z. Binti Ahmad, "Markov CA, multi regression, and multiple decision making for modeling historical changes in Kirkuk city, Iraq," *Journal of the Indian Society of Remote Sensing*, vol. 42, no. 1, pp. 165–178, 2014.
[56] J. Eastman, *IDRISI Selva Manual*, Clark Labs, Clark University, Worcester, MA, USA, Version 17.01, 2012.
[57] S. K. Singh, S. Mustak, P. K. Srivastava, S. Szabó, and T. Islam, "Predicting spatial and decadal LULC changes through cellular automata Markov chain models using earth observation datasets and geo-information," *Environmental Processes*, vol. 2, no. 1, pp. 61–78, 2015.
[58] A. I. Abdulrahman and S. A. Ameen, "Predicting Land use and land cover spatiotemporal changes utilizing CA-Markov model in Duhok district between 1999 and 2033," *Academic Journal of Nawroz University*, vol. 9, no. 4, pp. 71–80, 2020.
[59] Y. Wang and X. Zhang, "A dynamic modeling approach to simulating socioeconomic effects on landscape changes," *Ecological Modelling*, vol. 140, no. 1-2, pp. 141–162, 2001.
[60] G. R. Pontius and J. Malanson, "Comparison of the structure and accuracy of two land change models," *International Journal of Geographical Information Science*, vol. 19, no. 2, pp. 243–265, 2005.
[61] A. Mohamed and H. Worku, "Simulating urban land use and cover dynamics using cellular automata and Markov chain approach in Addis Ababa and the surrounding," *Urban Climate*, vol. 31, Article ID 100545, 2020.
[62] V. A. Parsa, A. Yavari, and A. Nejadi, "Spatio-temporal analysis of land use/land cover pattern changes in Arasbaran Biosphere Reserve: Iran," *Modeling Earth Systems and Environment*, vol. 2, no. 4, pp. 1–13, 2016.
[63] M. E. Hasan, B. Nath, A. H. M. R. Sarker et al., "Applying multi-temporal Landsat satellite data and markov-cellular automata to predict forest cover change and forest degradation of Sundarban reserve forest, Bangladesh," *Forests*, vol. 11, no. 9, p. 1016, 2020.
[64] M. Camara, "Integrating cellular automata Markov model to simulate future land use change of a tropical basin," *Global Journal of Environmental Science and Management*, vol. 6, no. 3, pp. 403–414, 2020.
[65] P. Subedi, K. Subedi, and B. Thapa, "Application of a hybrid cellular automaton-Markov (CA-Markov) model in land-use change prediction: a case study of saddle creek drainage basin, Florida," *Applied Ecology and Environmental Sciences*, vol. 1, no. 6, pp. 126–132, 2013.
[66] S. Kumar, N. Radhakrishnan, and S. Mathew, "Land use change modelling using a Markov model and remote sensing," *Geomatics, Natural Hazards and Risk*, vol. 5, no. 2, pp. 145–156, 2014.
[67] M. D. Behera, S. N. Borate, S. N. Panda, P. R. Behera, and P. S. Roy, "Modelling and analyzing the watershed dynamics using Cellular Automata (CA)-Markov model-a geo-information based approach," *Journal of Earth System Science*, vol. 121, no. 4, pp. 1011–1024, 2012.
[68] V. Mishra, P. Rai, and K. Mohan, "Prediction of land use changes based on land change modeler (LCM) using remote sensing: a case study of Muzaffarpur (Bihar), India," *Journal of the Geographical Institute Jovan Cvijic, SASA*, vol. 64, no. 1, pp. 111–127, 2014.
[69] R. G. Pontius Jr, "Comparison of categorical maps," *Photogrammetric Enginnering Remote Sensing*, vol. 66, pp. 1011–1016, 2000.
[70] R. G. Pontius Jr and L. C. Schneider, "Land-cover change model validation by an ROC method for the Ipswich watershed," *Agriculture, Ecosystems & Environment*, vol. 85, no. 1-3, pp. 239–248, 2001.
[71] H. M. Mosammam, J. T. Nia, H. Khani, A. Teymouri, and M. Kazemi, "Monitoring land use change and measuring urban sprawl based on its spatial forms," *The Egyptian Journal of Remote Sensing and Space Science*, vol. 20, no. 1, pp. 103–116, 2017.
[72] A. Shiferaw and K. Singh, "Evaluating the land use and land cover dynamics in Borena Woreda south Wollo highlands, Ethiopia," *Ethiopian Journal of Business and Economics (The)*, vol. 2, no. 1, 2011.
[73] J. S. Rawat and M. Kumar, "Monitoring land use/cover change using remote sensing and GIS techniques: a case study of Hawalbagh block, district Almora, Uttarakhand, India," *The Egyptian Journal of Remote Sensing and Space Science*, vol. 18, no. 1, pp. 77–84, 2015.
[74] K. Islam, M. Jashimuddin, B. Nath, and T. K. Nath, "Land use classification and change detection by using multi-temporal remotely sensed imagery: the case of Chunati wildlife sanctuary, Bangladesh," *The Egyptian Journal of Remote Sensing and Space Science*, vol. 21, no. 1, pp. 37–47, 2018.
[75] E. E. Hassen and M. Assen, "Land use/cover dynamics and its drivers in Gelda catchment, Lake Tana watershed, Ethiopia," *Environmental Systems Research*, vol. 6, no. 1, p. 4, 2018.
[76] G. B. Rossman and S. F. Rallis, *Learning in the Field: An Introduction to Qualitative Research*, Sage, Thousand Oaks, CF, USA, 2011.
[77] P. R. Ulin, E. T. Robinson, and E. E. Tolley, *Qualitative Methods in Public Health: A Field Guide for Applied Research*, John Wiley & Sons, Hoboken, NJ, USA, 2012.
[78] J. H. Frey and A. Fontana, "The group interview in social research," *The Social Science Journal*, vol. 28, no. 2, pp. 175–187, 1991.
[79] E. E. Tolley, P. R. Ulin, N. Mack, E. T. Robinson, and S. M. Sucoop, *Qualitative Methods in Public Health: A Field Guide for Applied Research*, John Wiley & Sons, Hoboken, NJ, USA, 2016.
[80] W. G. Cochran, *Sampling Techniques*, John Wiley & Sons, Hoboken, NJ, USA, 1977.
[81] A. A. Central Statistics Agency, *Ethiopia, Summary and Statistical Report of the 2007. Population and Housing Census: Population Size by Age and Sex*, Central Statistics Agency, Ethiopia, 2007.
[82] T. M. Lillesand, R. W. Kiefer, and J. Chipman, *Remote Sensing and Image Interpretation*, JohnWiley and Sons Inc, New York, NY, USA, 2004.
[83] H. E. Getachew and A. M. Melesse, "The impact of land use change on the hydrology of the Angereb watershed, Ethiopia," *International Journal of Water Sciences*, vol. 1, no. 6, 2012.
[84] S. Hailemariam, T. Soromessa, and D. Teketay, "Land use and land cover change in the Bale Mountain Eco-Region of Ethiopia during 1985 to 2015," *Land*, vol. 5, no. 4, p. 41, 2016.
[85] A. K. Tilahun, "Land use land cover change and its implication on surface runoff: a case study of Baro river basin in south western Ethiopia," *Journal of Environmental Earth Science*, vol. 5, no. 8, 2015.

[86] W. Bewket, "Land cover dynamics since the 1950s in Chemoga watershed, Blue Nile basin, Ethiopia," *Mountain Research and Development*, vol. 22, no. 3, pp. 263–269, 2002.
[87] A. González-Robles, A. J. Manzaneda, T. Salido et al., "Spatial genetic structure of a keystone long-lived semiarid shrub: historical effects prevail but do not cancel the impact of recent severe habitat loss on genetic diversity," *Conservation Genetics*, vol. 21, no. 5, pp. 853–867, 2020.
[88] A. Romero-Muñoz, G. Fandos, A. Benítez-López, and T. Kuemmerle, "Habitat destruction and overexploitation drive widespread declines in all facets of mammalian diversity in the Gran Chaco," *Global Change Biology*, vol. 27, pp. 755–767, 2020.
[89] P. Cabral and A. Zamyatin, "Markov processes in modeling land use and land cover changes in Sintra-Cascais, Portugal," *Dyna*, vol. 76, no. 158, pp. 191–198, 2009.
[90] G. Vázquez-Quintero, R. Solís-Moreno, M. Pompa-García, F. Villarreal-Guerrero, C. Pinedo-Alvarez, and A. Pinedo-Alvarez, "Detection and projection of forest changes by using the Markov chain Model and cellular automata," *Sustainability*, vol. 8, no. 3, p. 236, 2016.
[91] M. W. A. Halmy, P. E. Gessler, J. A. Hicke, and B. B. Salem, "Land use/land cover change detection and prediction in the north-western coastal desert of Egypt using Markov-CA," *Applied Geography*, vol. 63, pp. 101–112, 2015.
[92] C. Liping, S. Yujun, and S. Saeed, "Monitoring and predicting land use and land cover changes using remote sensing and GIS techniques—a case study of a hilly area, Jiangle, China," *PLoS One*, vol. 13, no. 7, p. e0200493, 2018.
[93] K. Li, M. Feng, A. Biswas, H. Su, Y. Niu, and J. Cao, "Driving factors and future prediction of land use and cover change based on satellite remote sensing data by the LCM model: a case study from Gansu province, China," *Sensors*, vol. 20, no. 10, p. 2757, 2020.
[94] G. Tian, J. Duan, and L. Yang, "Spatio-temporal pattern and driving mechanisms of cropland circulation in China," *Land Use Policy*, vol. 100, p. 105118, 2020.
[95] F. Imad, Z. Anis, and M. Mohamed, "Assessment of the effects of land use/land cover changes on soil loss and sediment yield using WaTEM/SEDEM model: case study of ziz upper watershed in SE-Morocco," *Current Applied Science and Technology*, vol. 21, pp. 334–347, 2020.
[96] M. Woube, *Effects of Resettlement Schemes on the Biophysical and Human Environments: The Case of the Gambela Region, Ethiopia*, Universal-Publishers, Irvine, CF, USA, 2005.
[97] S. Pausewang, F. Cheru, S. Brune, and E. Chole, *Ethiopia-rural Development Options*, Zed Books, London, UK, 1990.
[98] I. Tamrat, "Governance of large scale agricultural investments in Africa: the case of Ethiopia," in *Proceedings of World Bank Conference on Land Policy and Administration*, Washington, DC, USA, April 2010.
[99] M. M. Mekonnen and A. Y. Hoekstra, "Four billion people facing severe water scarcity," *Science Advances*, vol. 2, no. 2, Article ID e1500323, 2016.
[100] B. Yonas, F. Beyene, L. N. Gebreyes, and A. Angassa, "Influence of resettlement on pastoral land use and local livelihoods in southwest Ethiopia," *Tropical and Subtropical Agroecosystems*, vol. 16, no. 1, pp. 103–117, 2013.